Dynamical phase transitions in ultracold chemistry

Vijay Ganesh Sadhasivam[1,3], Fumika Suzuki[1,2], Bin Yan[1,2], Nikolai Sinitsyn[1]

[1]Theoretical Division, Los Alamos National Laboratory, Los Alamos, 87545, New Mexico, USA.

[2]Center for Nonlinear Studies, Los Alamos National Laboratory, Los Alamos, 87545, New Mexico, USA.

[3]Yusuf Hamied Department of Chemistry, University of Cambridge, Lensfield road, Cambridge, CB2 1EW, UK.

Contributing authors: vgs23@cam.ac.uk; fsuzuki@lanl.gov; byan@lanl.gov; nsinitsyn@lanl.gov;

Abstract

Advances in ultracold chemistry have demonstrated the possibility of coherent conversion of ultracold (fermionic and bosonic) atoms into molecules, including the reactions between completely bosonic condensates. Central to these conversions is a dynamical phase transition (DPT) induced by association of atoms at a Feshbach resonance. Here we show that interactions between the formed molecules can introduce fundamental changes in the physics around the Feshbach resonance including a change in the order of the phase transition, yield of the reaction, the coherent oscillations between atoms and molecules following the adiabatic transition through the resonance, and the formation of a molecular squeezed and cat states. We present a theoretical model that accounts for these interactions and quantifies the number of nonadiabatic excitations, along with the Kibble-Zurek scaling laws for the nonadiabatic effects in various regimes of this model.

Keywords: Ultracold chemistry, Quantum superchemistry, Quantum Phase transitions, Kibble-Zurek mechanism

1 Introduction

Tuning a magnetic field across the Feshbach resonance drives an ultracold atomic system through a quantum critical point and the phase transition [1, 2] of the conversion between the atoms and molecules. This reaction is quantum coherent and reversible at macroscopic scale. The time-dependent *Tavis-Cummings (TC) model* [3] is the minimal model that captures many nontrivial many-body effects that encounter during the stimulated reaction. Its Hamiltonian is

$$\hat{H}_{TC}(t) = -\beta t \hat{\psi}^\dagger \hat{\psi} + g(\hat{\psi}^\dagger \hat{S}^- + \hat{\psi}\hat{S}^+) \tag{1}$$

Here, $S \gg 1$ is the quantum mechanical spin, and β is the *sweep rate* of the transition through the Feshbach resonance. The sweep rate is controllable experimentally in a broad range – from very fast to the quasi-adiabatic values. The bosonic operator, $\hat{\psi}^\dagger$, creates a molecule. The *pseudo-spin* raising and lowering operators, $\hat{S}^+$ and $\hat{S}^-$, correspond to, respectively, dissociation of a molecule and association of two fermionic atoms to form a bosonic molecule with a characteristic coupling g (see [4, 5] for derivation of this model from true atomic-molecular Hamiltonians). The driven TC model can also be reformulated in terms of a fully bosonic reaction between bosonic atomic and molecular condensates [4, 5]. We will focus here on the reaction in which there are no molecules initially, and the fermions are initially in the degenerate Fermi sea. This corresponds in (1) to the initial state, as $t \to -\infty$, without the molecules and the spin fully up-polarized along the z-axis.

The time-dependent sweep is needed in practice to make all atoms encounter the resonance. In addition, the quantum adiabatic theorem guarantees that a sufficiently slow sweep converts the initially atomic state into the bosonic ground state, which is the molecular condensate. Hence, potentially, a 100% efficiency of the reaction is possible. However, the true adiabatic limit cannot be reached, so it is particularly important to understand the quasiadiabatic regime with small but finite β. This regime is characterized by the number of *nonadiabatic excitations*, n_{ex}, which is the number of atomic pairs that did not form the molecule after the transition through the resonance, i.e., as $t \to +\infty$.

An unusual theoretical finding about the time-dependent TC model was the discovery of its integrability [6, 7], which proved the existence of a dynamic phase transition and confirmed the semiclassical predictions for the power-law scaling of the nonadiabatic excitation density after the quasi-adiabatic sweep through the resonance [4]. Despite the success of this solvable model, its key theoretical predictions remain to be verified experimentally. Moreover, recent experiments with a bosonic reaction show a behavior that is not known within the slowly driven TC model, such as the emergence of the coherent oscillations between atoms and molecules after crossing the Feshbach resonance and a pre-thermalization in the atomic-molecular mixture state.

One possibility to extend the TC model to account for this rich behavior is to add a dispersion of the atomic states. This results in a generalized TC model [5, 7] that, surprisingly, is also solvable but leading to essentially the same predictions for the behavior of the nonadiabatic excitations on the sweep rate as the minimal model (1). Hence, other interaction types may be needed to explain the rich observed behavior.

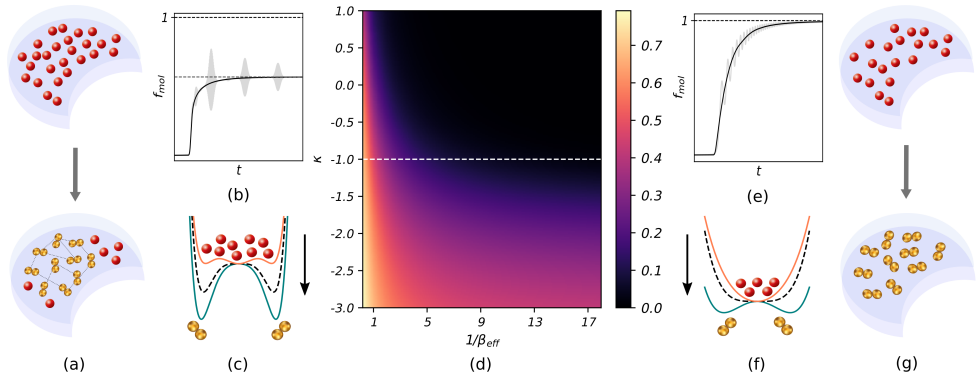

Fig. 1: An ultracold atomic reaction undergoing, respectively, (a-b-c) the first-order and (e-f-g) the second-order dynamical phase transition. (a) For the 1st order, both molecules and atoms can be in the local energy minima simultaneously, whereas (g), for the 2nd order, a high efficiency of the chemical reaction can be achieved by an adiabatic transition between the molecular and atomic energy minima. (b) and (e) The numerically obtained time-dependent fraction of the atoms converted to molecules during a qusi-adiabatic transition through, respectively, the first-order and the second-order critical points. The Hamiltonian for simulations is in Eq. (2) with an extra interacting term (2). (c) and (f) The mean-field ground energy as a function of the order parameter in the first-order and second-order dynamical phase transition, respectively (arrows show the direction of time) (d) The numerically obtained phase diagram describing the dependence of the number of nonadiabatic excitations, $n_{\rm ex}$, as a function of the inverse transition rate (x-axis) and the molecular interaction strength, $\kappa = r/g$ in Eq. (2), (y-axis). For the generalized Tavis-Cummings model, $\kappa = -1$ separates the regimes with 1st ($\kappa < -1$) and 2nd ($\kappa > -1$) order phase transitions. This explains the fast increase of the number of excitation numbers below the $\kappa = -1$ line.

In this article, we consider a different generalization of the model (1), in which we add another nonlinear interaction term

$$\hat{H}_{\rm int} := r(\hat{\psi}^\dagger\hat{\psi})^2 = r\hat{n}^2, \tag{2}$$

(where $\hat{n}$ is the molecular number operator) to get:

$$\hat{H}(t) = \hat{H}_{TC}(t) + H_{\rm int} \tag{3}$$

This interaction at the Feshbach resonance is effectively broadening the molecular dispersion energy, which becomes now dependent on the number of molecules that changes during the reaction. This interaction must be present in ultracold molecules due to dipole interactions and elastic scatterings.

We find that this addition to the model does lead to a substantially richer physical behavior, especially for the quasi-adiabatic transitions. This could be anticipated from the TC model applications in optics, where such a nonlinear term describes the optical mode in a 'Kerr-like' medium, showing many new effects, such as the second-harmonic generation [8–10].

With this addition, the phase diagram for the reaction depends both on the sweep rate β and the nonlinearity r. In Fig. 1d we show the result of our numerical simulations for the number of the nonadiabatic excitations following the sweep of the chemical potential. By setting $r = \kappa g$, the line $\kappa = -1$ marks a critical nonlinearity, such that for $\kappa < -1$ the number of the nonadiabatic excitations is much larger than for $\kappa > -1$, especially in the quasi-adiabatic limit (large $1/\beta_{\rm eff}$). We will show that this behavior follows from the possibility of either 2nd or 1st order phase transition during the sweep through the Feshbach resonance. Our model is no longer exactly solvable but in the quasi-adiabatic limit it leads to the analytical structure that can be studied in detail. Thus, we will provide the scaling laws for the number of the nonadiabatic excitations. We will also show that even during the adiabatic transition through the resonance, the system shows oscillations of the atomic-molecular population (observed in [11]). We also predict a complicated collapse and revival pattern for such oscillations in certain regimes of the interaction strengths.

2 Results

2.1 Semiclassical description and phase transitions

Our interest is in potentially large maximal number of molecules $N = 2S \gg 1$ that can be created during the sweep through the resonance. This limit justifies application of the semiclassical approximation. First, we note that our model conserves

$$N := \hat{\psi}^\dagger \hat{\psi} + \frac{1}{2}(\hat{I} + \hat{S}_z). \tag{4}$$

Hence, it is convenient to mark all states only by the number of molecules:

$$|n\rangle \equiv |n\rangle_m \otimes |S-n\rangle_{S_z},$$

where $|n\rangle_m$ is the state with n molecules and $|S-n\rangle_{S_z}$ is the spin state with $S_z = S-n$. The initial state as $t \to -\infty$ corresponds to $|n\rangle = |0\rangle$. The matrix elements $\langle n|\hat{H}_{TC}|m\rangle$ in this basis are given by

$$H_{nm} = -\beta t n\, \delta_{n,m} + gn\sqrt{N-n+1}\, \delta_{n,m-1} + g(n+1)\sqrt{N-n}\, \delta_{n,m+1}. \tag{5}$$

Let us look for the solution of the Schrödinger equation in the form $|\psi\rangle = \sum_{n=0}^{N} a_n(t)|n\rangle$, and introduce the amplitude generating function

$$u(\phi, t) = \sum_{n=0}^{N} a_n(t) e^{in\phi}. \tag{6}$$

Note that $na_n e^{in\phi} = -ia_n \partial e^{in\phi}/\partial\phi$, so the time-dependent Schrödinger equation for the amplitudes can be written in terms of a single equation for $u(\phi, t)$ as

$$i\frac{\partial}{\partial t}u(\phi,t) = \hat{H}\left(-i\frac{\partial}{\partial\phi}, \phi\right) u(\phi,t), \tag{7}$$

where we associate $\hat{n} \equiv -i\partial/\partial\phi$. In the semiclassical approximation we can then associate ϕ with a coordinate that is conjugated to the classical momentum n. In addition, we can disregard the terms of the order $1/N$. Then, the classical Hamiltonian that corresponds to the Schrödinger equation (7) has the form

$$H_{cl}(n, \phi; \gamma) = \gamma n + \frac{r}{\sqrt{N}}n^2 + 2gn\sqrt{N-n}\cos(\phi) \tag{8}$$

with a time-dependent parameter

$$\gamma = \gamma(t) = -\beta t,$$

and the classical equations of motion

$$\frac{d\phi}{dt} = \frac{\partial H_{cl}}{\partial n}, \quad \frac{dn}{dt} = -\frac{\partial H_{cl}}{\partial \phi}. \tag{9}$$

2.2 Quasi-adiabatic second order phase transition

Up to the new r-dependent nonlinear term, this Hamiltonian coincides with the analogous semiclassical Hamiltonian in [4]. The relation between the classical variables and the number of the nonadiabatic excitations is established by noting that as $t \to \pm\infty$ the time-dependent term completely dominates: $H_{cl} \sim \gamma n$. Following [4], we note that the equations of motion initially conserve n and the adiabatic invariant is given by the initial number of molecules, $n_{-\infty}$:

$$I_- = \frac{1}{2\pi}\int_0^{2\phi} n\, d\phi = n_{-\infty},$$

If during the evolution the adiabatic invariant acquires a small contribution ΔI, this is interpreted as the number of the nonadiabatic excitations, i.e, $n_{ex} = \Delta I$, and the number of the created molecules is given by

$$n_{+\infty} = N - \Delta I - I_-.$$

We should assume that initially $n_{-\infty} \sim 1$. The next approximation can be justified by assuming a nearly adiabatic sweep of the chemical potential [4]. The point $\phi^* = \pi$ is a steady point of the classical equations, in which vicinity the system evolves during the quasi-adiabatic evolution. Assuming that near this point $n \ll N$, and retaining the

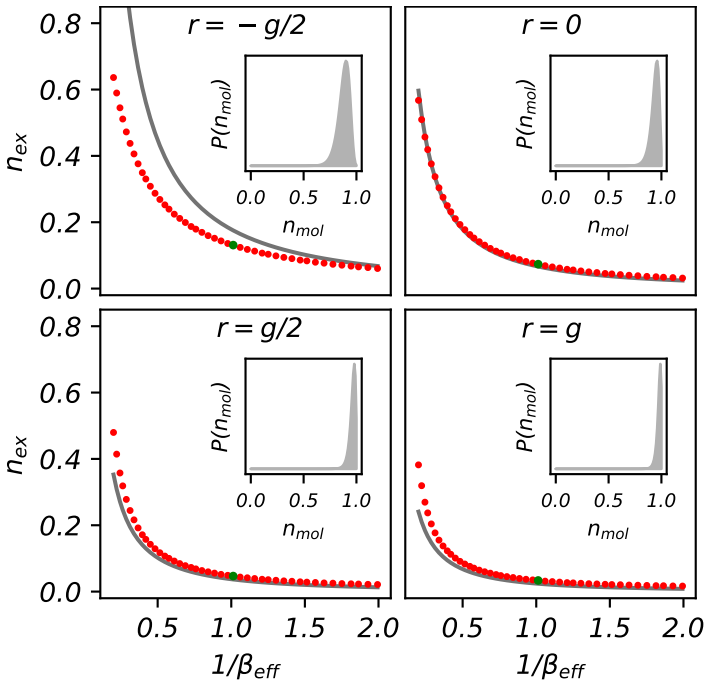

Fig. 2: Dependence of the number $n_{\rm ex}$ of excitations on the sweeping rates for different values of κ in the case of a second-order DPT. Inset: Distribution of molecule number in the limit $t \to \infty$.

terms of the lowest order we find an effective Hamiltonian that governs the evolution at the early stage of the reaction.

$$H_{cl}(n,\phi;\gamma) \approx \left(\gamma - 2g\sqrt{N}\right) n + \left(\frac{r+g}{\sqrt{N}}\right) n^2 + g\sqrt{N} n\phi^2. \tag{10}$$

For a quasi-adiabatic evolution, the nonadiabatic excitations are generally suppressed exponentially, as $\Delta I \sim \exp(-a/\beta)$, with some finite positive a. Such excitation are not essential and we can safely disregard them. However, according to the Kibble-Zurek phenomenology, the excitations are enhanced near a critical point, at which the symmetry of the original ground state breaks down spontaneously. It turns out that the Hamiltonian (10) contains this event, so it is sufficient to describe the phase transition quantitatively.

For simplicity, we shift the zero of time by setting:

$$s = t + 2g\beta\sqrt{N}, \tag{11}$$

and define a generalized position and momentum coordinates by the canonical transformation in (10):

$$Q = \sqrt{n}, \quad P = -2\sqrt{n}\phi, \tag{12}$$

and get an effective one-dimensional Hamiltonian:

$$H^{II}_{eff}(Q, P, s) := -\beta s\, Q^2 + \left(\frac{r+g}{\sqrt{N}}\right) Q^4 + \left(\frac{g\sqrt{N}}{2}\right) \frac{P^2}{2}, \tag{13}$$

where now P is treated as the momentum and Q is the coordinate.

Suppose that $r + g > 0$. This corresponds to either repulsive ($r > 0$) or weakly attractive ($-g < r < 0$) interactions between the formed molecules. If s were a constant, then the Hamiltonian (13) would describe a nonlinear oscillator with the potential energy

$$V(Q) = -\beta s\, Q^2 + \left(\frac{r+g}{\sqrt{N}}\right) Q^4. \tag{14}$$

The initial conditions correspond to $Q \sim 1$. In fact, a quantum mechanical treatment of the initial conditions needs averaging of the behavior over a distribution of small initial values with $0 < Q \ll N$ [4]. However, we will use a trick that avoids this step. The 2nd order phase transition encounters at $s = 0$. Indeed, for $x < 0$, the potential $V(Q)$ has a single minimum at $Q = 0$ but for $s > 0$, there are two local minima at $Q_{min} \sim \pm\sqrt{\beta N s/(r+g)}$.

As the time variable s changes across $s = 0$, the system undergoes a second-order phase transition, as illustrated in Fig. 1f. That is, for $s < 0$, the system is initially near a single minimum but it has to fall into one of the new minima for $s > 0$. In the phase space, this corresponds to crossing a caustic, at which the adiabatic invariant is no longer conserved. Thus, our approximations are justified because they capture the main source of the nonadiabatic excitations.

The evolution equations for Q and P with the Hamiltonian (10), acquire a universal form after the rescaling of the variables:

$$s \to \lambda s, \quad Q \to uQ, \quad P \to vY,$$

and

$$H_{\text{eff}} \to \lambda H_{\text{eff}}(\lambda s, uQ, vP)/(uv),$$

where λ, u, and v are constants. We choose them so that H_{eff} in terms of the rescaled variables has the form with only numerical coefficients

$$H = -s\frac{Q^2}{2} + \frac{Q^4}{2} + \frac{P^2}{2}. \tag{15}$$

In the new variables, the equations of motion have the canonical form of the Painlevé-II equation

$$\frac{d^2Q}{ds^2} = sQ - 2Q^3. \tag{16}$$

The dynamics does not depend anymore on the relative values of the parameters r and g. However, we reiterate that at $r = 0$, the model is exactly solvable, so all known facts about the solution of the driven TC model can now be applied to the dynamics according to Eq. (16). Moreover, Eq. (16) has known asymptotics. Thus, if as $t \to -\infty$ the adiabatic invariant is $\mathcal{I}_-$, then the change of this invariant as $t \to +\infty$ is given by

$$\Delta\mathcal{I} = \frac{1}{2\pi} \log_e \left(e^{-2\pi\mathcal{I}_-} - 1 \right) \tag{17}$$

The rescaling of variables, however, is not canonical, so it does not conserves the action:

$$\frac{1}{2\pi} \int_0^{2\pi} n \, d\phi = \frac{uv}{2\pi} \oint P \, dQ.$$

Hence, if I is the adiabatic invariant in the original variables, n and ϕ, then in the rescaled Q and P the invariant is given by $\mathcal{I} = I/(uv)$. In our case

$$uv = \frac{\beta}{g^2 + gr}. \tag{18}$$

By restoring the adiabatic invariant in the original variables we find

$$\Delta I = \frac{\beta}{2\pi g(g+r)} \log_e \left(e^{-2\pi g(g+r)\mathcal{I}_-/\beta} - 1 \right).$$

This is interpretted as the number of the nonadiabatic excitations. Hence, the number of the created molecules is then $n(t\infty) \sim N - \Delta I$.

Here, $\mathcal{I}_-$ is still a free parameter. It is tempting to set it to be the value of the adiabatic invariant at the potential minimum of the model (15). As $t \to -\infty$, this corresponds to the minimum of the Harmonic oscillator, for which the Bohr quantization predicts $\mathcal{I}_- = 1/2$. However, our approximations leading to the model (15) formally apply for $1 \ll n$. Forturnately, we can use the fact that the for the solvable case with $r = 0$ the entire probability distribution of the created molecules is known analytically. Thus, for the position of the peak of this distribution the exact solution predicts that $\mathcal{I}_- = 1$. Moreover, both the semiclassical studies of Eq. (16) and the exact solution at $r = 0$ have shown that due to the large width of this distribution the average value of the number of molecules is slightly shifted from the probability maximum.

Given that all such corrections appear at early stages of evolution, for which the nonlinear effects are not essential, we expect that the same subdominant corrections apply to $r \neq 0$ case. We find then for the average number of excitations

$$\langle n_{ex} \rangle = \frac{\beta}{2\pi g(g+r)} \left[\log_e \left(e^{-2\pi g(g+r)\beta} - 1 \right) + C_\gamma \right], \tag{19}$$

where $C_\gamma \approx 0.5772$ is the Euler constant.

Note that this result is obtained from the exactly solvable case at $r = 0$ by merely rescaling the coupling as

$$g^2 \to g^2 + gr. \tag{20}$$

for a general value of r despite the original Hamiltonian does not have this property.

A comparison of these numerical results and the analytical formula (19) is shown in fig. 2. From fig. 2, we also infer that the analytical formula (19) is in better agreement with the numerical results in the same limit where $n_{\rm ex} \approx 0$. We attribute this to the change in the width of the molecule number distribution $P(n)$ following the sweep as a function of the effective sweeping rate $\beta_{\rm eff}$. Far from the adiabatic limit and close to $\kappa = -1$, we get a rather broad distribution (see inset of fig. 2) $P(n)$ which results in a breakdown of the semiclassical approximations that led to the derivation of (19). For $\kappa \leq -1$, the system no longer undergoes a second-order phase transition, so we don't expect any of the results derived in this section to hold.

One of the defining features of the nonadiabatic transformation following the following a forward sweep is the presence of *transient nonadiabatic oscillations* (gray curve in fig. 1e) of molecular population which has been experimentally observed in both fermionic and bosonic [11] reactions. In [11], the frequency of these oscillations exhibited a distinct power law dependence on the number of atoms at the start. This was attributed to bosonic stimulation of the ultracold reaction, referred to as 'quantum superchemistry'. Such features are characteristic of the nonadiabatic (or near-adiabatic regime). However, in the adiabatic limit, the molecular population smoothly increases in time and lead to a total conversion of atoms into molecules (see fig. 4d).

While the discussions in this section address the forward sweep, the same results also hold for the backward sweep except for the fact that the criteria for a second-order DPT shall be $r + g < 0$ instead. This can be easily seen by analyzing the Hamiltonian (3) by setting $t \to -t$.

2.3 First-order phase transition

For $r + g \leq 0$, the mean-field Hamiltonian in (10) is no longer stable and we hence need to include the additional hexic term in (14) to compute the appropriate tunneling probability. Assuming a similar shift of the zero of time in (11) and using the canonical transformation in (12), we get the following asymptotic Hamiltonian for $r + g < 0$:

$$H^I_{MF}(Q, P, s) := -\beta s\, Q^2 + \left(\frac{r+g}{\sqrt{N}}\right) Q^4 + \left(\frac{g}{4N^{3/2}}\right) Q^6 + \left(\frac{g\sqrt{N}}{2}\right) \frac{P^2}{2} \tag{21}$$

For a finite sweeping rate $\beta > 0$, we can compute the nonadiabatic tunneling probability (and hence $n_{\rm ex}$) from the dependence of the frequency ω_* of the fixed point (n_*, ϕ_*). At the critical point or crossover point $r = -g$, we obtain an exact analytical expression (derived in the methods section) for $n_{\rm ex}$ as a function of the effective

sweeping rate β_{eff}:

$$n_{\text{ex}} \sim \beta_{\text{eff}}^{2/3} \tag{22}$$

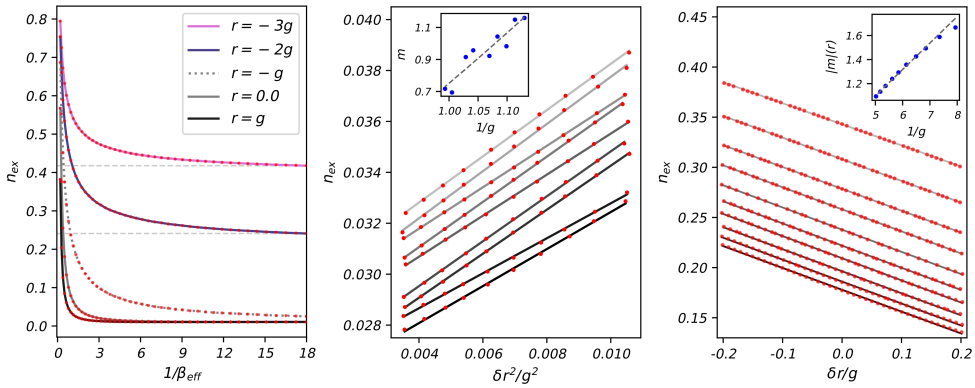

Fig. 3: (a) Dependence of the number n_{ex} of defective excitations on the effective sweeping rate for different values of κ. (b) Asymptotic dependence of n_{ex} on the nonlinearity in the *adiabatic* limit for different values of coupling g. Inset: Dependence of the slope of the n_{ex} curves on g. The dashed curve corresponds to a fit wrt $g^{-3/2}$ according to (24). (c) Asymptotic dependence of n_{ex} on the nonlinearity for the *near-adiabatic* case for different values of g. Inset: Dependence of the slope of the n_{ex} curves on g. The dashed curve corresponds to a linear fit wrt $1/g$ according to (25).

Thus, at the critical point $r_c = -g$, the model in (3) follows a Kibble-Zurek scaling law with the exponent $2/3$ and $n_{\text{ex}} \to 0$ in the limit $\beta_{\text{eff}} \to 0$ (see fig. 3a). For the parameter regime $r+g < 0$ (in the forward sweep) however, the system in (3) undergoes a (strictly) *first-order* phase transition (see fig. 1c). The defining characteristic of a first-order phase transition is the existence of a non-zero concentration of defective excitations n_{ex} even in the adiabatic limit [12]. A precise analytical formula exists for n_{ex} which can derived from a mean-field theoretic approach as in the previous section:

$$n_{\text{ex}}(\beta_{\text{eff}} \to \infty) \sim \frac{(r+g)^2}{g^{3/2}} N^{5/4} \tag{23}$$

(see methods section) Such an effect has been numerically observed in the nonlinear Landau-Zener model [12] and theoretical origins of this effect in the model (3) are also the same: the presence of unusual eigenvalue structure near the region $\gamma = 0$ in (8) (minus the constant shift in (11)) that prevents 'level crossings' even in the adiabatic limit $\beta_{\text{eff}} \to 0$.

The dependence of $n_{\rm ex}$ on $\beta_{\rm eff}$ for different values of r with $r < r_c$ (or $\kappa < -1$) are plotted in fig. 3b, clearly demonstrating non-zero defect concentrations below r_c in the adiabatic limit. We note that the concentration of defects increases steeply as:

$$n_{\rm ex}(\delta r) \sim \frac{\delta r^2}{g^{3/2}} \tag{24}$$

below the critical point (here $\delta r = r - r_c$). We hence expect $n_{\rm ex}$ to become increasingly higher with stronger attractive interactions between the formed molecules.

We also note (from fig. 1d) that the increased number of defects is not particularly specific to the adiabatic regime. Even in the near adiabatic or nonadiabatic regime ($\beta_{\rm eff} > 0$), the defect concentration is higher in the case of a first-order DPT compared to a second-order DPT, for a fixed atom-molecule coupling g. About the critical point $r = r_c$, there is a sharp decrease in $n_{\rm ex}$ as a function of δr:

$$n_{\rm ex}(\delta r) \sim -\frac{\delta r}{g} \tag{25}$$

(derived in the methods section). We plot the dependence of $n_{\rm ex}$ on δr (and on g) in the nonadiabatic limit in fig. 3c. Eq. (25) together (24) explains the sharp transition in $n_{\rm ex}$ observed around $\kappa = -1$ in fig. 1d.

2.4 Characterizing the first-order phase transition

The transient oscillations observed in the second-order DPT in the near-adiabatic (or nonadiabatic) limit is also observed for the first-order DPT, although they are severely damped (see shaded gray curve in fig. 1b). However, the main dynamical feature of the first-order DPT (apart from the existence of nonzero excitations in the adiabatic limit) is the generation of a broad distribution of molecular number states, denoted as $P(n_{\rm mol})$ in fig. 4c.

The presence of a broad number distribution $P(n_{\rm mol})$ leads to a complex *collapse* and *revival* of the molecular wavepacket following the forward sweep. This pattern of collapses and revivals are particularly prominent in the adiabatic limit and occur in a timescale comparable to the 'reaction time', i.e. the timescale of the forward sweep. They are rather suppressed in the near-adiabatic case where the transient nonadiabatic oscillations remain undamped by the collapse of the molecular wavepacket. Such patterns are rather familiar as they have been studied extensively in the time-independent versions of the Jaynes-Cummings model [13], Bose-Hubbard model [14], a model of nonlinear directional couplers [15] and even in a generalized version [16] of the atom-field interaction model in [11].

However, the driving the nonlinear Tavis-Cummings model (3) across a quantum-phase transition through a linear sweep, allows us to *selectively* obtain these oscillations by tuning the interaction strength to enable a first-order DPT. These oscillations are absent in the case of the second-order DPT since it produces a sharply-peaked number distribution in the adiabatic limit.

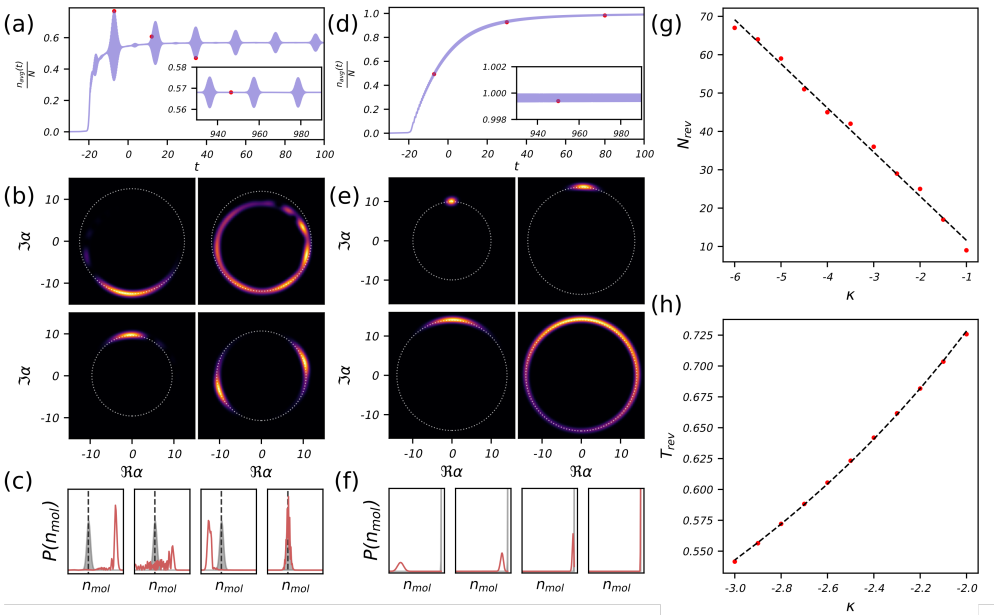

Fig. 4: (a) Plot of $\langle n_{\rm mol}\rangle$ vs time for $k = -3$, i.e. for first-order DPT in the adiabatic limit. Inset: Dependence of $\langle n_{\rm mol}\rangle$ with t in the long-time limit. (b)Coherent projection of the molecular wavefunction at the times marked in red dots in (a) (left to right in (a) corresponds to left-right-top-bottom in (b)). (c) Plots of number distribution of molecules for the times marked in (a) (from left to right). (d) Same as in (a), but for the second-order DPT with $\kappa = 0$. (e) Same as in (b), but with $\kappa = 0$. (f) Same as in (c), but with $\kappa = 0$. (g) Plot of number of revivals in a given time window for different values of κ in the first-order DPT regime (same g, adiabatic limit), fit to a linear curve (dashed line). (h) Time period of a particular revival as a function of κ fit to $T_{\rm rev} \sim 1/|\kappa|$ (dashed line).

The projection of the time-dependent molecular wavefunction onto a basis of coherent states is plotted in fig. 4b. It can be observed that the collapse and revival patterns constitutes an oscillation of the number distribution $P(n_{\rm mol})$ about the asymptotic limit (marked in gray in fig. 4c). We note that these collapse-revival patterns are also found in the case of backward sweep for the first-order phase transition (although $r_c = g$ instead). We also find that the number $N_{\rm rev}$ of revivals per unit time increases linearly with the strength of nonlinearity ($|\kappa|$) for the first-order DPT. The frequency of the collapse-revival patterns decreases gradually following the sweep and and in general saturates to a constant value resulting in a punctuated series of revivals that survive for a very long time. The time-period $T_{\rm rev}$ of any particular collapse and revival pair also decreases with $|\kappa|$ as:

$$T_{\rm rev} \sim \frac{1}{|\kappa|} \tag{26}$$

We plot the dependence of $N_{\rm rev}$ and $T_{\rm rev}$ on κ in fig. 4g.

It is to be emphasized that (as is known from [14]) this collapse-revival pattern is purely quantum-mechanical phenomenon; the semiclassical Hamiltonian in (8) does not exhibit these features. One of the main indicators of this inherently quantum feature of the dynamics is the generation of a *squeezed cat state* in the $t \to \infty$ limit of the forward sweep (see fig. 4b). This again, is specific to the first-order DPT; the second-order DPT creates a phase-smeared distribution due to the number-phase uncertainty relation [17]), sharply peaked around $n_{\rm mol} = N$ where N is the number of starting atoms (see fig. 4e and 4f).

3 Discussion

We have thus presented a comprehensive description of the role of molecular interactions in mediating DPTs in ultracold chemistry. We also impress upon the fact that the scaling laws and analytical predictions following from the dynamics of the mean-field Hamiltonians (8),(10) and (21) are universal and similar universal behaviour can be observed in any 0+1-dimensional field theory with an action functional of the form:

$$S = \int dt \, \left[(\partial_t \Phi)^2 - V(\Phi) \right] \tag{27}$$

where $V(\Phi)$ describes a double-well potential (see also [18]):

$$V(\Phi) = -\beta t \Phi^2 + \frac{g_4 \Phi^4}{4} + \frac{g_6 \Phi^6}{6} \tag{28}$$

(truncated at order 4 or 6 depending on the sign of the term g_4). We also expect that the collapse and revival pattern shown in fig. 4b to be universal since it is a result of a broad distribution of the quantum wavepacket following a first-order DPT.

The presence of the collapse-revival oscillations also indicate the generation of a *prethermalized* state following a first-order DPT. Such states have been observed in the nonequilibrium dynamics following a sudden quench in the Bose-Hubbard [19] and Fermi-Hubbard model [20] in previous studies. These states are 'quasisteady' and carry a long-term memory of their initial conditions (following the quench), which is in stark contradiction with their nonintegrability.

The prethermalized states have been characterized by their relaxation to a nonequilibrium (or non-thermal) value of number occupancy and a complex series of collapse and revival patterns [20] following the quench (which is observed for the first-order DPT as shown in fig. 4b). The time-period of these revivals were also found to be inversely related to the interaction strength (as in (26)). Experimental signatures of this collapse-revival patterns were first observed (to the best of our knowledge) in the landmark experiments of Greiner et al [21] on ultracold bosonic atoms in an optical lattice (see also [22] for a more recent review on this topic).

While many of these properties were attributed to be a result of using a sudden quench (as in [19, 20]), in our model (3), we observe them in the *adiabatic* limit of

extremely gradual quench. We hence expect that experiments in ultracold chemistry which convert atoms into molecules (with many-body interactions) by driving them along a magnetic field ramp (of varying steepness), to be an ideal testbed for exploring the nature of such prethermalized states.

We also expect our study to have potential impact on the endeavours in creating non-classical states in bosonic systems such as the macroscopic cat states and squeezed states. In the past, several experiments have targeted the creation of such non-classical states [23–25], some of which indeed used a Kerr-type nonlinearity to stabilize these states. Such states are of utmost importance in quantum sensing and metrology [26].

In molecules, we expect such nonlinear contributions to arise naturally from dipolar interactions and lead to the generation of squeezed cat states when the interaction strength matches the realm of the first-order DPT. The main experimental challenge will be in tuning the interaction strength and obtaining the desired degree of quantum control. With major strides of experimental development in ultracold chemistry, we expect this to be possible in the near future.

Appendix A Methods

A.1 Propagation of the TDSE

The time-dependent Schrödinger equation that describes the time evolution of the Hamiltonian (3) was propagated using a trotter-factorized discretization of the unitary propagator. Since (3) is also sparse (as is evident from (5)), the time complexity of the cost of the propagation scales linearly with the number of starting atoms N. The coherent Husimi Q projection of the wavefunction in the molecule number basis (fig. 4) was obtained as:

$$Q(\alpha) = \frac{1}{\pi}|\langle\alpha|\psi_{\mathrm{mol}}\rangle|^2 \tag{A1}$$

$$\langle\alpha|\psi_{\mathrm{mol}}\rangle = e^{-|\alpha|^2/2}\sum_{n=0}^{N}\frac{\alpha^n\psi_{\mathrm{mol}}(n)}{\sqrt{n!}} \tag{A2}$$

where $Q(\alpha)$ corresponds to the projection onto a coherent state indexed by $|\alpha\rangle$ and $\psi_{\mathrm{mol}}(n)$ is the probability amplitude that the molecular wavefunction is in the state $|n\rangle$ with n molecules.

A.2 Tunneling probability: Second-order DPT

In the adiabatic limit, it is well known that the tunneling probability (and hence n_{ex}) can be computed from the adiabatic invariant [4, 27]:

$$I = \frac{1}{\pi}\int p(q)\,dq \tag{A3}$$

For the mean-field Hamiltonian (10), the canonical position and momentum variables are ϕ and n respectively. In a forward sweep, we have $I(t \to -\infty) = I_i = 0$, since $n(t \to -\infty) = 0$. If $n = \overline{n}$ at $t \to +\infty$ then, since the phase-space curves 'flatten out' [4],

$$I_f = 2\,\overline{n} \tag{A4}$$

Hence, we have:

$$\Gamma = I_f - I_i = \frac{\Delta I}{2} \tag{A5}$$

In general, the main change in the action occurs around the point of dynamical phase-transition $t = 0$. Now, consider the simplified Hamiltonian (10). Let's make scaling transformation:

$$s \to \lambda s, \quad X \to \alpha X, \quad Y \to \beta Y$$

and

$$H \to \lambda H(\lambda s, \alpha X, \beta Y)/(\alpha\beta).$$

with

$$\lambda = \frac{1}{b^{1/3}}, \quad \alpha = \frac{1}{a^{1/2}b^{1/6}}, \quad \beta = \frac{2}{a^{1/2}b^{5/6}} \tag{A6}$$

so that H takes the form

$$H = -s\frac{X^2}{2} + \frac{X^4}{2} + \frac{Y^2}{2}.$$

This transformation, however, is not canonical, so it does not conserves the action:

$$\frac{1}{2\pi}\int_0^{2\pi} n\,d\phi = \frac{\alpha\beta}{2\pi}\oint Y\,dX.$$

Hence, if I_- is the initial action in physical variables, then this action in variables X, Y is $\alpha\beta I_-$.

Exact solution allows us to fix I_-. If we set true $I_- = 2$, which agrees with exact solution, then the action in Painleve-II formulas should be

$$I_- = \frac{1}{\alpha\beta} = \frac{g^2 + gr}{2\beta}$$

At the end, we will have to return to old variables, so, we should say that we should convert the invariant back, so

$$\Delta I \to \Delta I \alpha\beta$$

This means that $\Delta I \to \frac{2\beta}{g^2}$. Since everything depends on I_- universally, we find that the expression for the number of produced particles in semiclassical limit is changed merely by replacing

$$g^2 \to \gamma^2 \equiv g^2 + gr.$$

For example, taking already known results for $r = 0$ and replacing there g with γ, we find that the normalized number of particles after the sweep, i.e. $\bar{n} \equiv n(+\infty)/N$, is given by

$$\bar{n} = 1 - \frac{\log_e(1-x)}{N \log_e x}, \quad x = e^{-2\pi\gamma^2/\beta}, \tag{A7}$$

where

$$\gamma^2 \equiv g^2 + gr.$$

A.3 First-order DPT

Adiabatic limit: In the limit of $\beta \to 0$, we can compute the adiabatic tunneling probability from (A5) as:

$$\Gamma = \frac{\Delta I}{2} = \frac{I_c}{2} \tag{A8}$$

where I_c is the action of the separatrix curve at the point of first-order DPT. For the mean-field Hamiltonian (21) which expressed in the form of a double-well potential (28), we can compute I_c as:

$$I_c = I = \frac{1}{\pi} \int_{Q_1}^{Q_2} P(Q)\, dQ \tag{A9}$$

where $Q_1 = 0, Q_2 = \pm\sqrt{3g_4/2g_6}$ are the turning points on the separatrix. Computing this yields:

$$I_c = \frac{3\sqrt{3}}{64} \frac{g_4^2}{g_6^{3/2}} \tag{A10}$$

Nonadiabatic case: When a Hamiltonian has a time-dependent perturbation γ, the nonadiabatic tunneling probability is computed from the change in the curvature (or frequency) ω_* [27] as:

$$\Gamma = \frac{\Delta I}{2} := -\Re \int_{-\infty}^{\infty} i e^{i\theta} \dot{\gamma}\, d\tau \frac{d\theta}{\omega_*(I,\gamma)} \tag{A11}$$

The standard procedure to evaluate the scaling behaviour of the above expression is to express ω_* in terms of θ [12]. In the case of the first-order DPT, the major change in the curvature occurs at the point $t = t_*$ (see (11)) after which n increases in time. We consider the dynamical equations given by the Hamiltonian (8) in terms of the scaled time variable $\tau = g\sqrt{N}t$ which yields:

$$\frac{d\overline{n}}{d\tau} = 2\overline{n}\sqrt{1-\overline{n}}\sin\phi := f_1(\overline{n},\phi) \tag{A12}$$

$$\frac{d\phi}{d\tau} = \overline{\gamma} + 2\kappa\overline{n} + \cos\phi \left(\frac{2-3\overline{n}}{\sqrt{1-\overline{n}}}\right) := f_2(\overline{n},\phi) \tag{A13}$$

where $\overline{\gamma} = \gamma/(g\sqrt{N}), \kappa = r/g$ and $\overline{n} = n/N$. It is straightforward to see that the rate of change of $\overline{\gamma}$ is given as:

$$\frac{d\overline{\gamma}}{d\tau} = \frac{\beta}{g^2 N} := \frac{\beta_{\text{eff}}}{\log N} \tag{A14}$$

we absorb the logarithmic term into β_{eff}. The reason for the inclusion of this term is explained in [5]: for a given β, the $f = 2\pi/\beta_{\text{eff}}$ is the point of discontinuity in the behaviour of n_{ex} vs β (see eq. 13 in [5]).

Around the fixed point $(\overline{n}_*, \phi_*) = (0, \pi)$, for $\kappa = -1$, this yields:

$$\omega_* \sim \overline{n}_* \tag{A15}$$

from which we get:

$$\omega_* \sim \beta_{\text{eff}}^{1/3} \theta^{1/3} \tag{A16}$$

This yields the following expressions:

$$\Gamma_c \sim -\beta_{\text{eff}}^{2/3} \tag{A17}$$

$$\Rightarrow n_{\text{ex},c} \sim \beta_{\text{eff}}^{2/3} \tag{A18}$$

which was numerically confirmed in fig. 3a.

For the near-critical case with $\kappa = -1 + \delta\kappa$, we get:

$$\omega_* \sim \left(\overline{n}_* + \frac{1}{3}\delta\kappa\right) \tag{A19}$$

Expanding upto linear order in κ, we get:

$$\Gamma = \Gamma_c + \Delta\Gamma_c \tag{A20}$$

where

$$\Delta\Gamma_c \sim \delta\kappa \tag{A21}$$

(we numerically found a weak dependence of $\Delta\Gamma_c$ with respect to β_{eff}). Note that the sign of Γ_c is positive: when κ increases, the tunneling probability goes up (which can be inferred from fig. 1d. For a constant g, we hence have:

$$n_{\text{ex}}(\delta r) \sim -\frac{\delta r}{g} \tag{A22}$$

Thus, the concentration of defective excitations increases linearly with $1/g$, which is also evident from fig. 1d and the inset in fig. 3c.

References

[1] Romans, M., Duine, R., Sachdev, S., Stoof, H.: Quantum phase transition in an atomic bose gas with a feshbach resonance. Physical review letters **93**(2), 020405 (2004)

[2] Radzihovsky, L., Park, J., Weichman, P.B.: Superfluid transitions in bosonic atom-molecule mixtures near a feshbach resonance. Physical review letters **92**(16), 160402 (2004)

[3] Yurovsky, V., Ben-Reuven, A., Julienne, P.S.: Quantum effects on curve crossing in a bose-einstein condensate. Physical Review A **65**(4), 043607 (2002)

[4] Altland, A., Gurarie, V., Kriecherbauer, T., Polkovnikov, A.: Nonadiabaticity and large fluctuations in a many-particle landau-zener problem. Physical Review A **79**(4), 042703 (2009)

[5] Malla, R.K., Chernyak, V.Y., Sun, C., Sinitsyn, N.A.: Coherent reaction between molecular and atomic bose-einstein condensates: integrable model. Physical Review Letters **129**(3), 033201 (2022)

[6] Sinitsyn, N.A., Li, F.: Solvable multistate model of landau-zener transitions in cavity qed. Physical Review A **93**(6), 063859 (2016)

[7] Sun, C., Sinitsyn, N.A.: Landau-zener extension of the tavis-cummings model: Structure of the solution. Physical Review A **94**(3), 033808 (2016)

[8] Bužek, V., Jex, I.: Dynamics of a two-level atom in a kerr-like medium. Optics Communications **78**(5-6), 425–435 (1990)

[9] Agarwal, G., Puri, R.: Collapse and revival phenomenon in the evolution of a resonant field in a kerr-like medium. Physical Review A **39**(6), 2969 (1989)

[10] Gora, P., Jedrzejek, C.: Nonlinear jaynes-cummings model. Physical Review A **45**(9), 6816 (1992)

[11] Zhang, Z., Nagata, S., Yao, K.-X., Chin, C.: Many-body chemical reactions in a quantum degenerate gas. Nature Physics, 1–5 (2023)

[12] Liu, J., Fu, L., Ou, B.-Y., Chen, S.-G., Choi, D.-I., Wu, B., Niu, Q.: Theory of nonlinear landau-zener tunneling. Physical Review A **66**(2), 023404 (2002)

[13] Shore, B.W., Knight, P.L.: The jaynes-cummings model. Journal of Modern Optics **40**(7), 1195–1238 (1993)

[14] Milburn, G., Corney, J., Wright, E.M., Walls, D.: Quantum dynamics of an atomic bose-einstein condensate in a double-well potential. Physical Review A **55**(6), 4318 (1997)

[15] Chefles, A., Barnett, S.M.: Quantum theory of two-mode nonlinear directional couplers. Journal of Modern Optics **43**(4), 709–727 (1996)

[16] Santos, G., Tonel, A., Foerster, A., Links, J.: Classical and quantum dynamics of a model for atomic-molecular bose-einstein condensates. Physical Review A **73**(2), 023609 (2006)

[17] Louisell, W.H.: Amplitude and phase uncertainty relations. Phys. Letters **7** (1963)

[18] Marino, J., Eckstein, M., Foster, M., Rey, A.-M.: Dynamical phase transitions in the collisionless pre-thermal statesof isolated quantum systems: theory and experiments. Reports on Progress in Physics (2022)

[19] Kollath, C., Läuchli, A.M., Altman, E.: Quench dynamics and nonequilibrium phase diagram of the bose-hubbard model. Physical review letters **98**(18), 180601 (2007)

[20] Eckstein, M., Kollar, M., Werner, P.: Thermalization after an interaction quench in the hubbard model. Physical review letters **103**(5), 056403 (2009)

[21] Greiner, M., Mandel, O., Hänsch, T.W., Bloch, I.: Collapse and revival of the matter wave field of a bose–einstein condensate. Nature **419**(6902), 51–54 (2002)

[22] Ueda, M.: Quantum equilibration, thermalization and prethermalization in ultracold atoms. Nature Reviews Physics **2**(12), 669–681 (2020)

[23] Kirchmair, G., Vlastakis, B., Leghtas, Z., Nigg, S.E., Paik, H., Ginossar, E., Mirrahimi, M., Frunzio, L., Girvin, S.M., Schoelkopf, R.J.: Observation of quantum state collapse and revival due to the single-photon kerr effect. Nature **495**(7440), 205–209 (2013)

[24] Ourjoumtsev, A., Kubanek, A., Koch, M., Sames, C., Pinkse, P.W., Rempe, G., Murr, K.: Observation of squeezed light from one atom excited with two photons. Nature **474**(7353), 623–626 (2011)

[25] Grimm, A., Frattini, N.E., Puri, S., Mundhada, S.O., Touzard, S., Mirrahimi, M., Girvin, S.M., Shankar, S., Devoret, M.H.: Stabilization and operation of a kerr-cat qubit. Nature **584**(7820), 205–209 (2020)

[26] Pirandola, S., Bardhan, B.R., Gehring, T., Weedbrook, C., Lloyd, S.: Advances in photonic quantum sensing. Nature Photonics **12**(12), 724–733 (2018)

[27] Landau, L.D., Lifshitz, E.M.: Mechanics and Electrodynamics. Elsevier, ??? (2013)